**Title: A derivation error exists in the current implementation of the Johnson et al. (1942) modified Arrhenius function that affects leaf carbon balance models**

**Running Title: Derivation error in modified Arrhenius model**

Author: Bridget Murphy[1], Joseph R. Stinziano[2,*]

Affiliations: [1] Department of Biology, University of Western Ontario, London, ON, Canada;

[2] Department of Biology, University of New Mexico, Albuquerque, NM, USA

[*] Corresponding author; Email: jstinziano@unm.edu; Tel: +1 (226) 678-1670

Article Type: Research Article

Word Count: 3,040

Introduction: 490

Material & Methods: 813

Results: 1154

Discussion: 557

Acknowledgments: 26

Number of Tables: 2

Number of Figures: 6

Supplementary Files: 1

**Abstract**

Understanding biological temperature responses is crucial to predicting global carbon fluxes. The current approach to modeling photosynthetic temperature responses in large scale modeling efforts uses a modified Arrhenius equation. We rederived the modified Arrhenius equation from the source publication and uncovered a missing term that was dropped between 1942 and 2002. We compare fitted temperature response parameters between the new and old derivation of the modified Arrhenius equation. We find that most parameters are minimally affected, though small errors still exist. We then scaled the impact of these small errors to whole plant carbon balance and found that the impact of the rederivation of the Arrhenius on modelled daily carbon gain causes a meaningful deviation of ~1.8%. This suggests that the error in the derivation of the modified Arrhenius equation has impacted predictions of carbon fluxes at larger scales. We argue that it is time to move beyond the modified Arrhenius paradigm since the current implementation is categorically incorrect and to use more thermodynamically-grounded temperature response equations going forward.

*Keywords: Arrhenius, temperature, photosynthesis, gas exchange, modeling, carbon balance*

## Introduction

Globally, photosynthesis and autotrophic respiration are the largest biological carbon fluxes, with photosynthesis removing ~120 Gt C year$^{-1}$ and autotrophic respiration releasing ~60 Gt C year$^{-1}$ (Amthor, 2000; Ciais et al., 2013). Given the temperature sensitivity of these large carbon fluxes, understanding how photosynthesis and respiration respond on acute, acclimatory, and adaptive timescales is crucial for predicting vegetative and carbon cycle responses to future global climates (Rogers et al., 2017; Stinziano et al. 2018). Biological temperature responses including photosynthesis and respiration are typically assumed to be exponential or peaked (Way and Yamori, 2014; Smith & Dukes, 2017; Kumarathunge et al., 2019). Exponential responses are usually modelled based on an Arrhenius-type curve (Arrhenius, 1915):

$$f(T) = Ae^{\frac{-E_a}{RT}} \quad \text{Equation 1}$$

$$f(T) = k_{25}e^{\left[\frac{E_a(T-298.15)}{RT298.15}\right]} \quad \text{Equation 2}$$

where f(T) is the rate of the process at temperature, A is a pre-exponential factor, T in K, $k_{25}$ is the rate of the process at 298.15 K, $E_a$ is the activation energy in J mol$^{-1}$, R is the universal gas constant of 8.314 J mol$^{-1}$ K$^{-1}$, and 298.15 is the reference temperature in K. As for peaked responses, while a few options are available (Kruse et al., 2008; Hobbs et al., 2013; Heskel et al., 2016), the most commonly implemented version is the modified Arrhenius model of Johnson et al. (1942) as presented in Medlyn et al. (2002):

$$f(T) = k_{25}e^{\left[\frac{E_a(T-298.15)}{RT298.15}\right]}\left[\frac{1+e^{\frac{298.15\Delta S-H_d}{298.15R}}}{1+e^{\frac{T\Delta S-H_d}{TR}}}\right] \quad \text{Equation 3}$$

where $H_d$ is the deactivation energy in J mol$^{-1}$, and ΔS is the entropy of the process in J mol$^{-1}$.

Equation 3 is used for modeling the temperature responses of photosynthetic capacity (based on Farquhar et al., 1980): maximum carboxylation capacity of rubisco, $V_{cmax}$, maximum electron transport capacity, $J_{max}$, and related kinetics as well as Sharkey (1985) and Harley & Sharkey (1991) in their

calculation of triose phosphate utilization capacity (TPU). These parameters are then used in ecophysiological studies to understand thermal acclimation of photosynthesis (see Kattge & Knorr, 2007; Smith & Dukes, 2017; and Kumarathunge et al., 2019 for examples). Furthermore, this equation is also used in terrestrial biosphere models to predict the future state of the Earth system (e.g. Rogers et al., 2017).

Due to its ubiquity, we revisited the original Johnson et al. (1942) modified Arrhenius function to rederive Equation 3. In the process of this rederivation, we uncovered a term that was dropped sometime between Johnson et al. (1942) and Medlyn et al. (2002) which causes a systematic error in the application of Equation 3 in calculations covering individual species (e.g. Medlyn et al., 2002) to global scale processes (e.g. Rogers et al., 2017). We then refit a freely available dataset (Kumarathunge et al., 2019), with both versions of the modified Arrhenius model, and fed the temperature response fits through a carbon balance model to estimate the impact of the derivation error on modelled plant carbon balance. We predicted that the derivation error would cause substantial variation in fitted temperature response parameters, and that these differences would propagate through to modelled daily carbon balance.

## Materials & methods

### Rederivation of the modified Arrhenius equation

Johnson et al. (1942, equation 24) describe the temperature response of the light intensity of a luciferase reaction as:

$$I = \frac{c'' T e^{\frac{-\Delta H‡}{RT}}}{1+e^{\frac{\Delta S}{R}} e^{\frac{-\Delta H}{RT}}} \qquad \text{Equation 4}$$

where I is the intensity of the luciferase reaction, c'' is not explicitly defined in Johnson et al. (1942), but presumably represents a second derivative of the rate, T is the temperature in K, R is the universal gas constant of 8.314 J $mol^{-1}$ $K^{-1}$, ΔH‡ is the activation energy in J $mol^{-1}$, ΔH is the deactivation energy in J $mol^{-1}$, and ΔS is the entropy in J $mol^{-1}$. We can relativize the equation to a reference temperature:

$$\frac{I}{I_{25}} = \frac{\frac{c'' T e^{\frac{-\Delta H‡}{RT}}}{1+e^{\frac{\Delta S}{R}} e^{\frac{-\Delta H}{RT}}}}{\frac{c''298.15 e^{\frac{-\Delta H‡}{R298.15}}}{1+e^{\frac{\Delta S}{R}} e^{\frac{-\Delta H}{R298.15}}}}$$ Equation 5

$$\frac{I}{I_{25}} = \frac{c'' T e^{\frac{-\Delta H‡}{RT}}}{c''298.15 e^{\frac{-\Delta H‡}{R298.15}}} \frac{1+e^{\frac{\Delta S}{R}} e^{\frac{-\Delta H}{R298.15}}}{1+e^{\frac{\Delta S}{R}} e^{\frac{-\Delta H}{RT}}}$$ Equation 6

$$\frac{I}{I_{25}} = \frac{T}{298.15} e^{\frac{-\Delta H‡}{RT} - \frac{-\Delta H‡}{R298.15}} \frac{1+e^{\frac{\Delta S}{R} + \frac{-\Delta H}{R298.15}}}{1+e^{\frac{\Delta S}{R} + \frac{-\Delta H}{RT}}}$$ Equation 7

$$I = I_{25} \frac{T}{298.15} e^{\left[\frac{-\Delta H‡298.15 - -\Delta H‡T}{RT298.15}\right]} \left[\frac{1+e^{\frac{298.15\Delta S + -\Delta H}{298.15R}}}{1+e^{\frac{T\Delta S + -\Delta H}{TR}}}\right]$$ Equation 8

$$I = I_{25} \frac{T}{298.15} e^{\left[\frac{\Delta H‡(T-298.15)}{RT298.15}\right]} \left[\frac{1+e^{\frac{298.15\Delta S - \Delta H}{298.15R}}}{1+e^{\frac{T\Delta S - \Delta H}{TR}}}\right]$$ Equation 9

Harmonizing the notation scheme to that typically used in plant ecophysiology:

$$f(T) = k_{25} \frac{T}{298.15} e^{\left[\frac{E_a(T-298.15)}{RT298.15}\right]} \left[\frac{1+e^{\frac{298.15\Delta S - H_d}{298.15R}}}{1+e^{\frac{T\Delta S - H_d}{TR}}}\right]$$ Equation 10

Note the difference between Equations 3 and 10: the term T / 298.15 is missing from Equation 3. This introduces multiple systematic errors:

1) fitted parameters $E_a$, $H_d$, and $\Delta S$;
2) scaling the rate variable using the wrong equation;
3) acclimation of $E_a$, $H_d$, and/or $\Delta S$ as errors due to 1) at each acclimation temperature.

Here we focus on the impact of 1 and 2 on modeling whole-plant carbon balance.

**Data analysis**

Using data from Kumarathunge et al. (2019), available from Kumarathunge et al. (2018), we fit Equations 3 and 10 to the data, both setting $H_d$ to 200 kJ mol$^{-1}$ and allowing $H_d$ to be fit. We used the

R package {minpack.lm} (Elzhov et al., 2016) with starting parameters of $E_a$ = 40 kJ $mol^{-1}$, ΔS = 0.650 kJ $mol^{-1}$, $k_{25}$ = mean(parameter), and $H_d$ (when fitted) varying from 1 to 500 kJ $mol^{-1}$, followed by the {BIC} function to select the best model based on Bayesian Information Criteria. We obtained 92 successful curve fits for the fixed $H_d$ case, and 84 successful curve fits for the fitted $H_d$ case. This allows us to explore the impact of the missing term on the output data under a typical fitting scenario ($H_d$ is fixed) and under the full fitting scenario.

**Modeling**

We modelled the impact of the equations 3 and 10 on daily net plant carbon balance under conditions of $H_d$ = 200 kJ $mol^{-1}$ and fitted $H_d$. Data for leaf area, root and shoot masses, as well as leaf dark respiration at 25 °C were taken for white spruce (*Picea glauca*) from Stinziano & Way (2017), while stomatal conductance model parameters were calculated with the gas exchange data reported in Stinziano & Way (2017). Mean data were taken from the control treatment at weeks 0 and 12 to provide contrasting biomass allocation patterns such that week 0 is a low respiration scenario and week 12 is a high respiration scenario. These different respiration scenarios were used to reduce bias in any conclusions regarding the impact of Equations 3 and 10 on carbon balance, as the ratio of photosynthesis to respiration may alter the sensitivity of carbon balance to the Arrhenius equation used. Root respiration for white spruce was taken from Weger and Guy (1991) and we assumed that stem respiration was equal to root respiration (Table 1).

**Table 1. Parameters used in modeling daily carbon gain.**

| Parameter | Group | Value | Reference |
|---|---|---|---|
| Respiration | $R_{dark}$ | 2.78 µmol $m^{-2}$ $s^{-1}$ | Stinziano & Way, 2017 |
| | $R_{day}$ | 0.7 * $R_{dark}$ | Ayub et al., 2011 |
| | $R_{root}$ | 0.0095 µmol $g^{-1}$ $s^{-1}$ | Weger & Guy, 1991 |
| | $R_{stem}$ | 0.0095 µmol $g^{-1}$ $s^{-1}$ | Assumed |
| | $Q_{10}$ | 2.015 | Atkin & Tjoelker, 2003 |
| Γ* | 25 °C | 42.75 µmol $mol^{-1}$ | Bernacchi et al., 2001 |
| | $E_a$ | 37.83 kJ $mol^{-1}$ | Bernacchi et al., 2001 |
| $K_m$ | 25 °C | 718.4 µmol $mol^{-1}$ | Bernacchi et al., 2001 |
| | $E_a$ | 65.51 kJ $mol^{-1}$ | Bernacchi et al., 2001 |
| α | | 0.8 | Norman & Campbell, 1998 |
| ϕ | | 0.08 | Norman & Campbell, 1998 |
| Leaf Area | Low R | 0.015 $m^2$ | Stinziano & Way, 2017 |
| | High R | 0.025 $m^2$ | Stinziano & Way, 2017 |

| | | | |
|---|---|---|---|
| Stem Mass | Low R | 0.496 g | Stinziano & Way, 2017 |
| | High R | 2.523 g | Stinziano & Way, 2017 |
| Root Mass | Low R | 0.498 g | Stinziano & Way, 2017 |
| | High R | 5.072 g | Stinziano & Way, 2017 |

**$Q_{10}$: thermal sensitivity coefficient; Γ*: photorespiratory $CO_2$ compensation point; $K_m$: Michaelis-Menten constant for rubisco; α: absorbance of photosynthetically activation radiation; ϕ: maximum quantum efficiency of photosynthetic electron transport; $E_a$: activation energy; $R_{dark}$: leaf respiration in the dark; $R_{day}$: leaf respiration in the light; $R_{root}$: root respiration; $R_{stem}$: stem respiration; Low R: low respiration scenario; High R: high respiration scenario.**

For the full model structure and equations, please see the accompanying R package {arrhenius.comparison} ("arrhenius.comparison_1.0.0.tar.gz"; Stinziano & Murphy, 2020) (see Table 2 for equations). Briefly, we linked the Medlyn et al. (2011) stomatal conductance model with the Farquhar et al. (1980) $C_3$ photosynthesis model, assuming infinite mesophyll conductance to $CO_2$ as these assumptions were used in fitting the data from Kumarathunge et al. (2018). Photosynthetic capacity, both maximum rubisco carboxylation capacity, $V_{cmax}$, and maximum electron transport rate, $J_{max}$ were scaled to temperature using either Equation 3 or 10, while respiration was scaled according to (Atkin & Tjoelker, 2003). Photosynthesis and respiration were summed across each modelled day to calculate daily plant carbon assimilation.

**Table 2. Equations used in modeling daily carbon uptake.**

| Equation | Reference |
|---|---|
| $f(T) = k_{25} Q_{10}^{\frac{T-298.15}{10}}$ | Atkin & Tjoelker, 2003 |
| $f(T) = k_{25} e^{\left[\frac{E_a(T-298.15)}{RT298.15}\right]}$ | Arrhenius, 1915 |
| $f(T) = k_{25} e^{\left[\frac{E_a(T-298.15)}{RT298.15}\right]} \left[\frac{1+e^{\frac{298.15\Delta S - H_d}{298.15R}}}{1+e^{\frac{T\Delta S - H_d}{TR}}}\right]$ | Johnson et al., 1942; Medlyn et al., 2002 |
| $f(T) = k_{25} \frac{T}{298.15} e^{\left[\frac{E_a(T-298.15)}{RT298.15}\right]} \left[\frac{1+e^{\frac{298.15\Delta S - H_d}{298.15R}}}{1+e^{\frac{T\Delta S - H_d}{TR}}}\right]$ | Johnson et al., 1942; this study |
| $W_c = V_{cmax} \frac{C_i - \Gamma*}{C_i + K_m}$ | Farquhar et al., 1980 |

| | |
|---|---|
| $W_j = min\left(J_{max}, \alpha\phi Q_{in}\frac{C_i - \Gamma*}{C_i + 2\Gamma*}\right)$ | Farquhar et al., 1980; Way et al., 2011 |
| $A_{gross} = min(W_c, W_j)$ | |
| $A_{net} = A_{gross} - R_{day}$ | |
| $g_s = g_0 + 1.6\left(1 + \frac{g_1}{\sqrt{VPD}}\right)\left(\frac{A_{net}}{C_a}\right)$ | Medlyn et al., 2011 |
| $C_i = C_a - 1.6\frac{A_{net}}{g_s}$ | |
| $A_{plant} = A_{net} \times LA - R_{dark} \times LA - R_{stem} \times SM - R_{root} \times RM$ | |
| $C_{balance} = \sum A_{plant} \times 3600 \times \frac{12.01}{1{,}000{,}000}$ | |

**f(T): rate of a process at a given temperature; T: temperature in K; $k_{25}$: rate of a process at 25 °C; $Q_{10}$: thermal sensitivity coefficient; $E_a$: activation energy in kJ mol$^{-1}$; ΔS: entropy parameter in kJ mol$^{-1}$; $H_d$: deactivation energy in kJ mol$^{-1}$; R: universal gas constant in 0.008314 kJ mol$^{-1}$ K$^{-1}$; $W_c$: rate of $CO_2$-limited carboxylation in µmol m$^{-2}$ s$^{-1}$; $W_j$: rate of RuBP regeneration-limited carboxylation in µmol m$^{-2}$ s$^{-1}$; $V_{cmax}$: maximum rate of rubisco carboxylation capacity in µmol m$^{-2}$ s$^{-1}$; $J_{max}$: maximum rate of electron transport in µmol m$^{-2}$ s$^{-1}$; $C_i$: intercellular $CO_2$ concentration in µmol mol$^{-1}$; Γ*: photorespiratory $CO_2$ compensation point in µmol mol$^{-1}$; $K_m$: Michaelis-Menten constant for rubisco in µmol mol$^{-1}$; α: absorbance of photosynthetically active radiation; ϕ: maximum quantum efficiency of electron transport; $Q_{in}$: incident photosynthetically active radiation; $A_{gross}$: gross $CO_2$ assimilation in µmol m$^{-2}$ s$^{-1}$; $A_{net}$: net $CO_2$ assimilation in µmol m$^{-2}$ s$^{-1}$; $R_{day}$: leaf day respiration in µmol m$^{-2}$ s$^{-1}$; $g_s$: stomatal conductance to water in mol m$^{-2}$ s$^{-1}$; $g_o$: intercept for the Medlyn et al. 2011 model; $g_1$: slope for the Medlyn et al. 2011 model; VPD: vapor pressure deficit in kPa; $C_a$: $CO_2$ concentration at the leaf surface in µmol mol$^{-1}$; $A_{plant}$: whole plant net $CO_2$ assimilation; LA: leaf area in m$^{-2}$; $R_{dark}$: leaf dark respiration in µmol m$^{-2}$ s$^{-1}$; $R_{stem}$: stem respiration in µmol m$^{-2}$ s$^{-1}$; $R_{root}$; root respiration in µmol m$^{-2}$ s$^{-1}$; SM: stem mass in g; RM: root mass in g; $C_{balance}$: whole plant daily carbon balance in g plant$^{-1}$ day$^{-1}$.**

Modeling was performed on 18 total days of environmental data, with three days of data from three months (17$^{th}$ – 19$^{th}$ of May, August, and October, 2019) obtained from external irradiance sensors at the Biotron Experimental Climate Change Research Centre at the University of Western Ontario and

the remaining environmental data from Environment Canada historical climate data for South London (43.01°N, 81.27°W, altitude: 251 m) and the rooftop greenhouse at the University of New Mexico (35.08°N, 106.62°W, altitude: 1587 m) to capture different levels of environmental variability (Fig. 1).

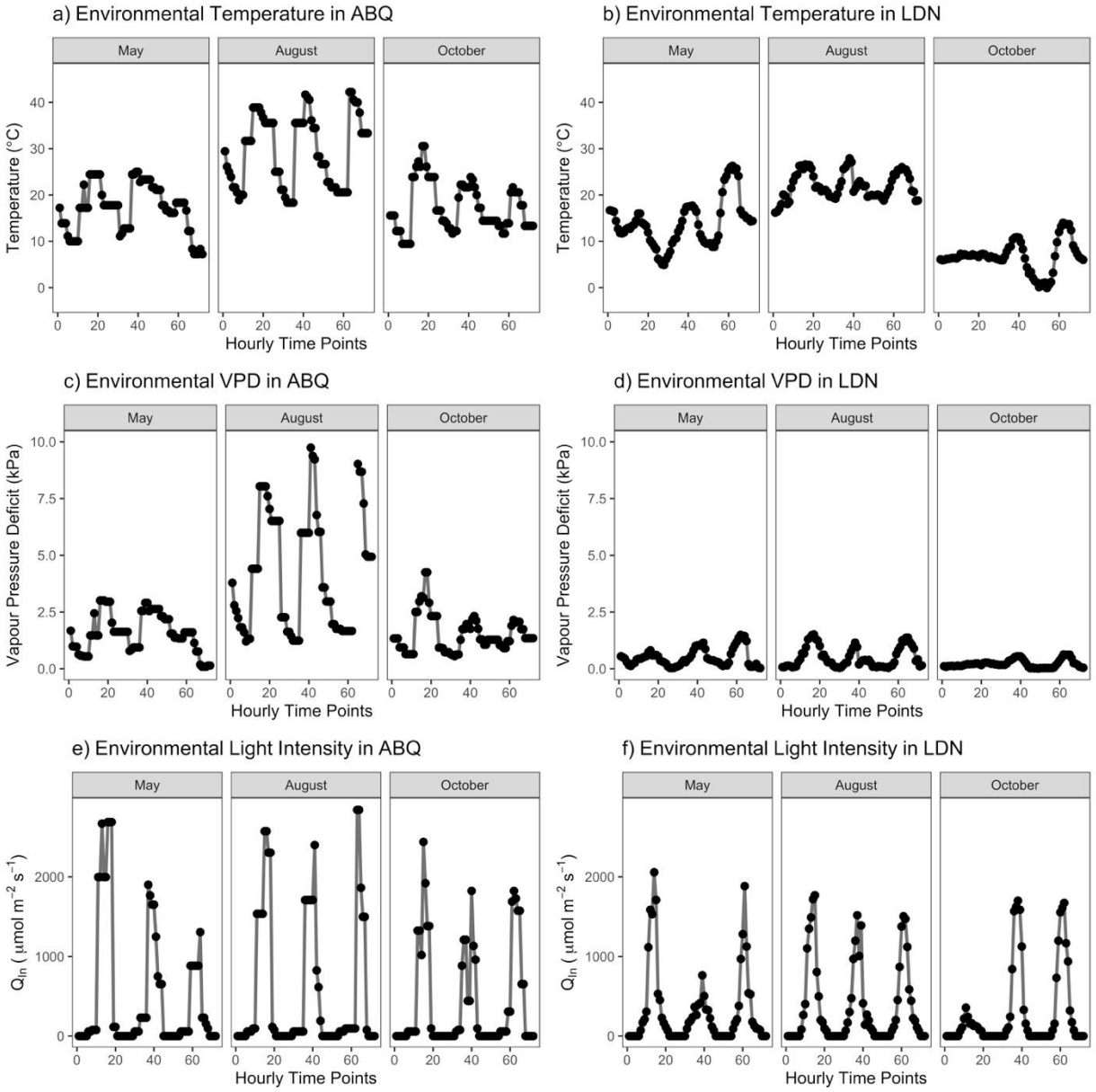


**Figure 1. Environmental data used to drive the model in Table 1 covering 3 days (17th, 18th, and 19th) of 3 months. (a,c,e) Albuquerque, NM, USA; (b,d,e) London, ON, Canada.**

Overall, the modeling approach allows us to assess the relative differences between Equations 3 and 10 under a low- and high- respiration scenario, fixing versus fitting $H_d$, and across different ranges of seasonal variability.

185

186 *Statistical analysis*

187 Data were analyzed using the {lm} function in R v.3.6.1 (R Core Team, 2019), regressing the data
188 obtained from Equation 10 against the data obtained from Equation 3. All code and data will be made
189 freely available on GitHub upon publication in the {arrhenius.comparison} R package (Stinziano &
190 Murphy, 2020).

191

192 **Results**

193 *Fixed $H_d$ of 200 kJ mol$^{-1}$*

194 Incorporating the missing term into Equation 3 to produce Equation 10 caused small differences in
195 the fitting of $E_a$ for $V_{cmax}$, with a slope of 0.997 ± 0.001 and intercept of -2.162 ± 1.19 · $10^{-1}$ kJ mol$^{-1}$
196 ($F_{1,90}$ = 4.56 · $10^5$, $R^2$ = 0.9998, $P$ < 2.2 · $10^{-16}$) (Fig. 2b). For ΔS, the slope was 0.991 ± 3 · $10^{-3}$ and an
197 intercept of 0.005 ± 2 · $10^{-3}$ kJ mol$^{-1}$ (intercept approximately 1% of fitted ΔS) ($F_{1,90}$ = 1.23 · $10^5$, $R^2$ =
198 0.9993, $P$ < 2.2 · $10^{-16}$) (Fig. 2f). Meanwhile $V_{cmax25}$ was identical between both approaches with a
199 slope of 1.000 ± 1.1 · $10^{-5}$ (intercept not significant; $F_{1,91}$ = 8.2 · $10^9$, $R^2$ = 1.000, $P$ < 2.2 · $10^{-16}$) (Fig. 3b).
200 For $J_{max}$, there were small differences in the fitting of $E_a$ for $J_{max}$, with a slope of 0.998 ± 2 · $10^{-3}$ and
201 intercept of -2.230 ± 1.08 · $10^{-1}$ kJ mol$^{-1}$ ($F_{1,91}$ = 3.3 · $10^5$, $R^2$ = 0.9997, $P$ < 2.2 · $10^{-16}$) (Fig. 2d). For ΔS,
202 the slope was 0.962 ± 3 · $10^{-3}$ and an intercept of 0.025 ± 2 · $10^{-3}$ kJ mol$^{-1}$ (intercept approximately 5%
203 of fitted ΔS) ($F_{1,90}$ = 1.1 · $10^5$, $R^2$ = 0.9992, $P$ < 2.2 · $10^{-16}$) (Fig. 2h). Meanwhile $J_{max25}$ was identical
204 between both approaches with a slope of 1.000 ± 1.2 · $10^{-5}$ (intercept not significant; $F_{1,92}$ = 6.7 · $10^9$,
205 $R^2$ = 1.000, $P$ < 2.2 · $10^{-16}$) (Fig. 3d).

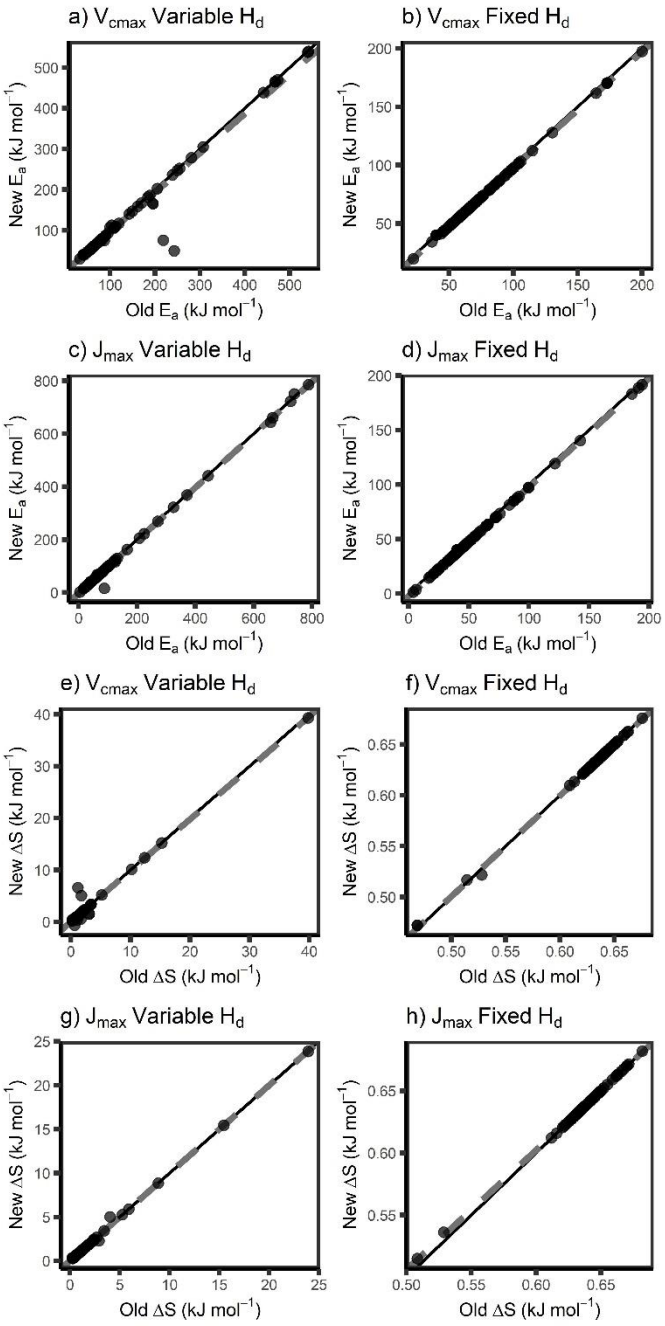


206

207 **Figure 2 – The modified Arrhenius equation with the missing term (Equation 10) gives**
208 **similar temperature response parameters as Equation 3 for $E_a$ (a-d) and ΔS (e-h) for both $V_{cmax}$ (a, b,**
209 **e, f) and $J_{max}$ (c, d, g, h) under scenarios where $H_d$ is allowed to vary (a, c, e, g) and is fixed to 200 kJ**
210 **mol$^{-1}$ (b, d, f, h). "New" indicates Equation 10, "Old" indicates Equation 3. $E_a$: activation energy, ΔS:**
211 **entropy parameter, $H_d$: deactivation energy, $V_{cmax}$: maximum capacity of rubisco carboxylation, $J_{max}$:**
212 **maximum rate of electron transport. Black line indicates 1:1 line and grey dashed line indicates**
213 **respective modeled slopes and intercepts.**

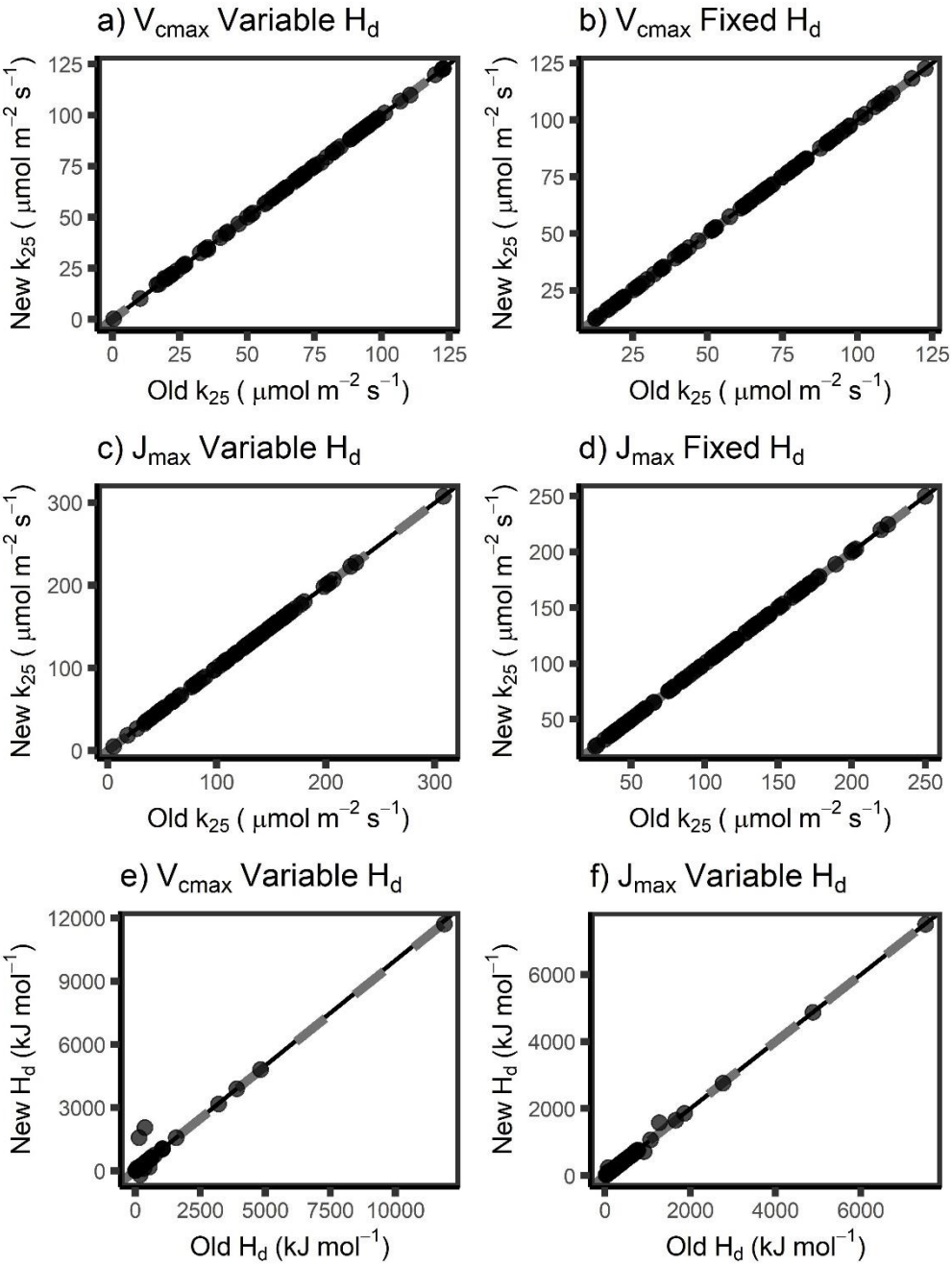


**Figure 3 – The modified Arrhenius equation with the missing term (Equation 10) gives similar temperature response parameters as Equation 3 for $k_{25}$ (a-d) and $H_d$ (e, f) for both $V_{cmax}$ (a, b, e) and $J_{max}$ (c, d, f) under scenarios where $H_d$ is allowed to vary (a, c, e, f) and is fixed to 200 kJ $mol^{-1}$ (b, d). "New" indicates Equation 10, "Old" indicates Equation 3. $k_{25}$: rate of the process at 25 °C, $H_d$: deactivation energy, $V_{cmax}$: maximum capacity of rubisco carboxylation, $J_{max}$: maximum rate of electron transport. Black line indicates 1:1 line and grey dashed line indicates respective modeled slopes and intercepts.**

*Variable $H_d$*

Incorporating the missing term into Equation 3 to produce Equation 10 caused small differences in the fitting of $E_a$ for $V_{cmax}$, with a slope of 0.966 ± 2.6 · $10^{-2}$ (intercept not significant; $F_{1,74}$ = 3005, $R^2$ = 0.976, $P < 2.2 \cdot 10^{-16}$) (Fig. 2a). For ΔS, the slope was 0.989 ± 1.7 · $10^{-2}$ (intercept not significant; $F_{1,74}$ = 3339, $R^2$ = 0.9783, $P < 2.2 \cdot 10^{-16}$) (Fig. 2e), while $H_d$ had a slope of 0.992 ± 1.9 · $10^{-2}$ (intercept not significant; $F_{1,74}$ = 2812, $R^2$ = 0.9744; $P < 2.2 \cdot 10^{-16}$) (Fig. 3e). Meanwhile $V_{cmax25}$ was nearly identical between both approaches with a slope of 1.000 ± 4 · $10^{-3}$ (intercept not significant; $F_{1,74} = 7.98 \cdot 10^6$, $R^2$ = 1.000, $P < 2.2 \cdot 10^{-16}$) (Fig. 3a). For $J_{max}$, there were small differences in the fitting of $E_a$ for $J_{max}$, with a slope of 1.000 ± 5 · $10^{-3}$ and an intercept of -3.119 ± 1.089 kJ $mol^{-1}$ ($F_{1,80} = 3.6 \cdot 10^4$, $R^2$ = 0.9978, $P < 2.2 \cdot 10^{-16}$) (Fig. 2c). ΔS was identical, the slope was 1.000 ± 4 · $10^{-3}$ (intercept not significant; $F_{1,81}$ = $6.4 \cdot 10^4$, $R^2$ = 0.9987, $P < 2.2 \cdot 10^{-16}$) (Fig. 2g), while $H_d$ was identical with a slope of 1.000 ± 4 · $10^{-3}$ (intercept not significant; $F_{1,81} = 5.2 \cdot 10^4$, $R^2$ = 0.9985; $P < 2.2 \cdot 10^{-16}$) (Fig. 3f). $J_{max25}$ was identical between both approaches with a slope of 1.000 ± 1 · $10^{-3}$ (intercept not significant; $F_{1,81} = 5.8 \cdot 10^7$, $R^2$ = 1.000, $P < 2.2 \cdot 10^{-16}$) (Fig. 3c).

*Impacts on modelled net carbon balance*

In general, the differences in thermal response parameters were amplified when integrated at the whole-plant level. For daily photosynthesis (A) measured at a fixed $H_d$ of 200 kJ $mol^{-1}$, the slope for the low respiration model was 0.977 ± 7.666 · $10^{-3}$ and an intercept of 0.002 ± 9.366 · $10^{-5}$ (approximately 2% of modeled A) ($F_{1,898} = 1.625 \cdot 10^6$, $R^2$ = 0.9994; $P < 2.2 \cdot 10^{-16}$) (Fig. 4b). Similarly, the high respiration model for A had a slope of 0.977 ± 7.666 · $10^{-3}$ and an intercept of 0.004 ± 1.591 · $10^{-3}$ (approximately 2% of modeled A) ($F_{1,898} = 1.625 \cdot 10^6$, $R^2$ = 0.9994; $P < 2.2 \cdot 10^{-16}$) (Fig. 4d). For daily A measured at a variable $H_d$, the slope for the low respiration model was 0.983 ± 9.909 · $10^{-3}$ and the intercept was 0.002 ± 1.128 · $10^{-3}$ (approximately 2% of modeled A) ($F_{1,556} = 9.834 \cdot 10^5$, $R^2$ = 0.9994; $P < 2.2 \cdot 10^{-16}$) (Fig. 4a). For the high respiration model of daily A, the slope was 0.983 ± 9.909 · $10^{-3}$ and the intercept was 0.003 ± 9.909 · $10^{-4}$ (approximately 2% of modeled A) ($F_{1,556} = 9.834 \cdot 10^5$, $R^2$ = 0.9994; $P < 2.2 \cdot 10^{-16}$) (Fig. 4c).

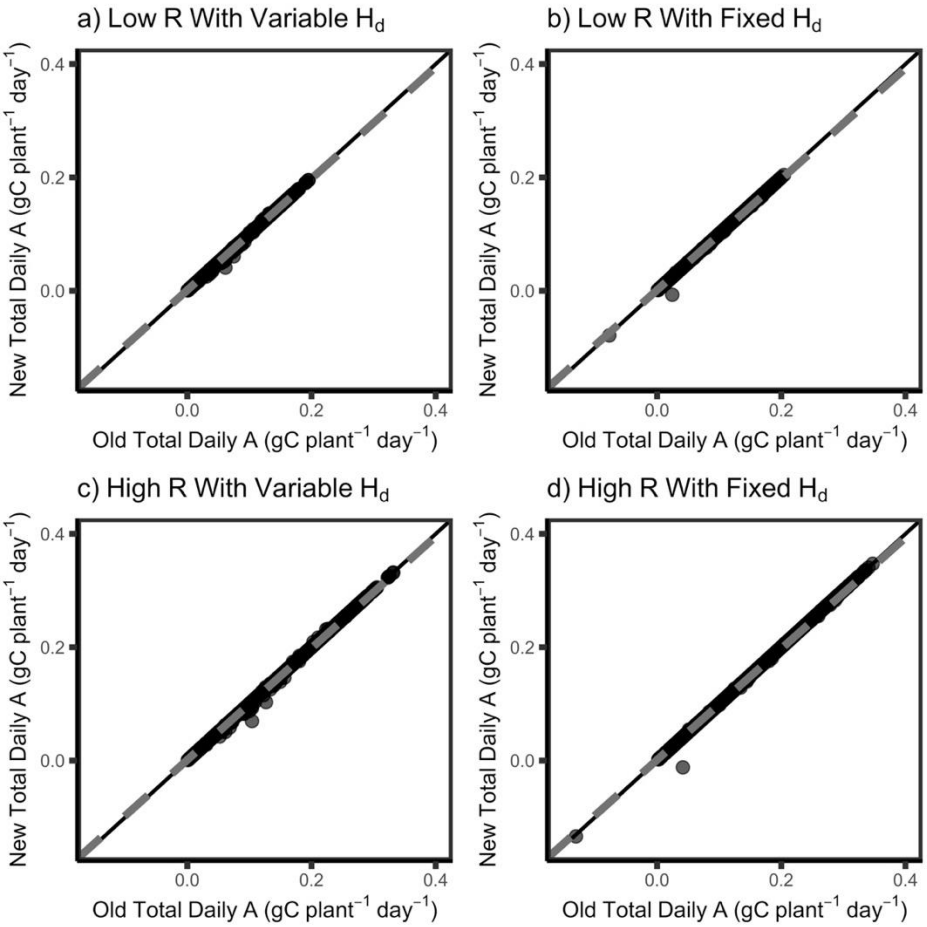


**Figure 4 – The modified Arrhenius equation with the missing term (Equation 10) gives slight differences in modeled total daily photosynthesis compared to Equation 3 for low R (a,b) and high R (c,d) under scenarios where $H_d$ is allowed to vary (a, c) and is fixed to 200 kJ mol$^{-1}$ (b,d). "New" indicates Equation 10, "Old" indicates Equation 3. A: photosynthesis, Low R: low respiration, High R: high respiration. Black line indicates 1:1 line and grey dashed line indicates respective modeled slopes and intercepts.**

The ratio of the total daily photosynthesis : respiration (A/R) was also considered when comparing models. Using a fixed $H_d$ of 200 kJ mol$^{-1}$, the low respiration model of A/R had a slope of 0.993 ± 5.634 · $10^{-3}$ and the intercept was 0.025 ± 0.002 (approximately 1% of modeled A/R) ($F_{1,898}$ = 3.109 · $10^6$, $R^2$ = 0.9997; $P$ <2.2 · $10^{-16}$) (Fig. 5b). The high respiration model of A/R was similar; the slope was 0.993 ± 5.628 and the intercept was 0.014 ± 0.001 (approximately 1% of modeled A/R) ($F_{1,898}$ = 3.115 · $10^6$, $R^2$ = 0.9997; $P$ <2.2 · $10^{-16}$) (Fig. 5d). Using a variable $H_d$, the low respiration model of A/R had a slope of 0.994 ± 0.001 and the intercept was 0.030 ± 0.001 (approximately 1% of modeled A/R) ($F_{1,556}$ = 6.857 ·

264 $10^5$, $R^2$ = 0.9992; $P$ <2.2 · $10^{-16}$) (Fig. 5a). The high respiration model had a similar slope of 0.994 ±

265 0.001 and the intercept was 0.017 ± 0.003 (approximately 1% of modeled A/R) ($F_{1,556}$ = 6.812 · $10^5$, $R^2$

266 = 0.9992; $P$ <2.2 · $10^{-16}$) (Fig. 5c).

267

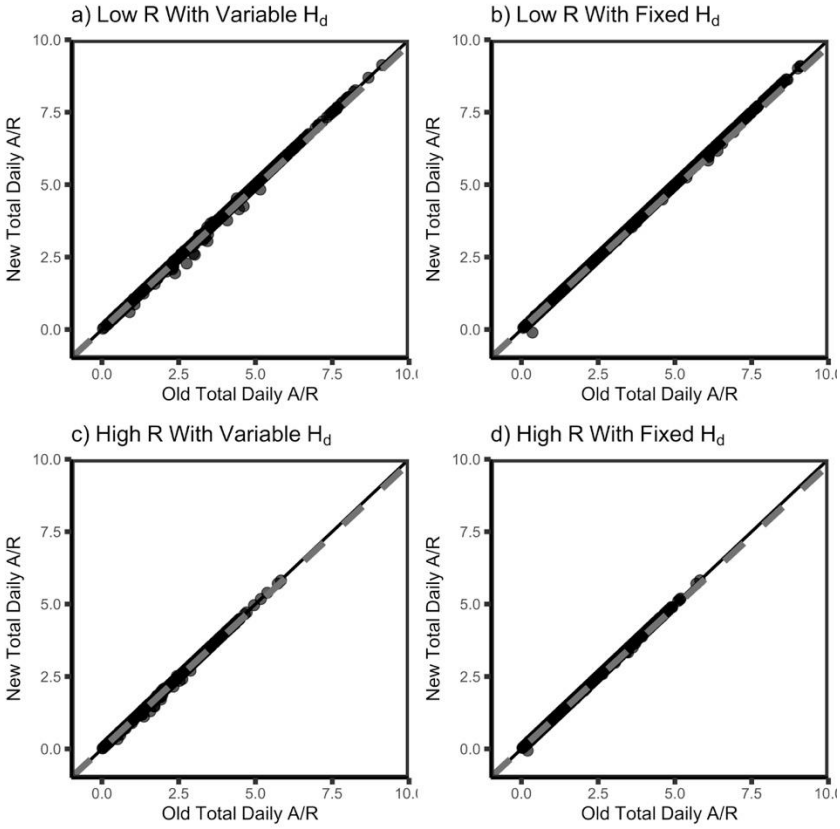


268

269 **Figure 5 – The modified Arrhenius equation with the missing term (Equation 10) gives slight**

270 **differences in modeled total daily A/R compared to Equation 3 for low R (a,b) and high R (c,d) under**

271 **scenarios where $H_d$ is allowed to vary (a, c) and is fixed to 200 kJ $mol^{-1}$ (b,d). "New" indicates**

272 **Equation 10, "Old" indicates Equation 3. A: photosynthesis, R: respiration, Low R: low respiration,**

273 **High R: high respiration. Black line indicates 1:1 line and grey dashed line indicates respective**

274 **modeled slopes and intercepts.**

275

276 Lastly, total daily carbon (C) gain was also compared between models with different thermal response

277 parameters. Using a fixed $H_d$ of 200 kJ $mol^{-1}$, the low respiration model of total C gain had a slope of

278 0.978 ± 7.445 · $10^{-4}$ and an intercept of 0.001 ± 7.609 · $10^{-5}$ (approximately 2% of modeled C gain)

279 ($F_{1,898}$ = 1.726 · $10^6$, $R^2$ = 0.9995; $P$ <2.2 · $10^{-16}$) (Fig. 6b). Likewise, the high respiration of total C gain

280 had a slope of 0.979 ± 7.261 · $10^{-4}$ and an intercept of 0.001 ± 1.116 · $10^{-4}$ (approximately 2% of

modeled C gain) ($F_{1,898}$ = 1.821 · $10^6$, $R^2$ = 0.9995; $P$ <2.2 · $10^{-16}$) (Fig. 6d). This can be compared to a variable $H_d$; starting with the low respiration model, total C gain had a slope of 0.985 ± 9.555 · $10^{-4}$ and an intercept of 0.001 ± 1.223 · $10^{-3}$ (approximately 1.5% of modeled C gain) ($F_{1,556}$ = 1.06 · $10^6$, $R^2$ = 0.9995; $P$ <2.2 · $10^{-16}$) (Fig. 6a). The high respiration of total C gain also had a slope of 0.985 ± 9.110 · $10^{-4}$ and an intercept of 0.001 ± 1.290 · $10^{-4}$ (approximately 1.5% of modeled C gain) ($F_{1,556}$ = 1.17 · $10^6$, $R^2$ = 0.9995; $P$ <2.2 · $10^{-16}$) (Fig. 6c).

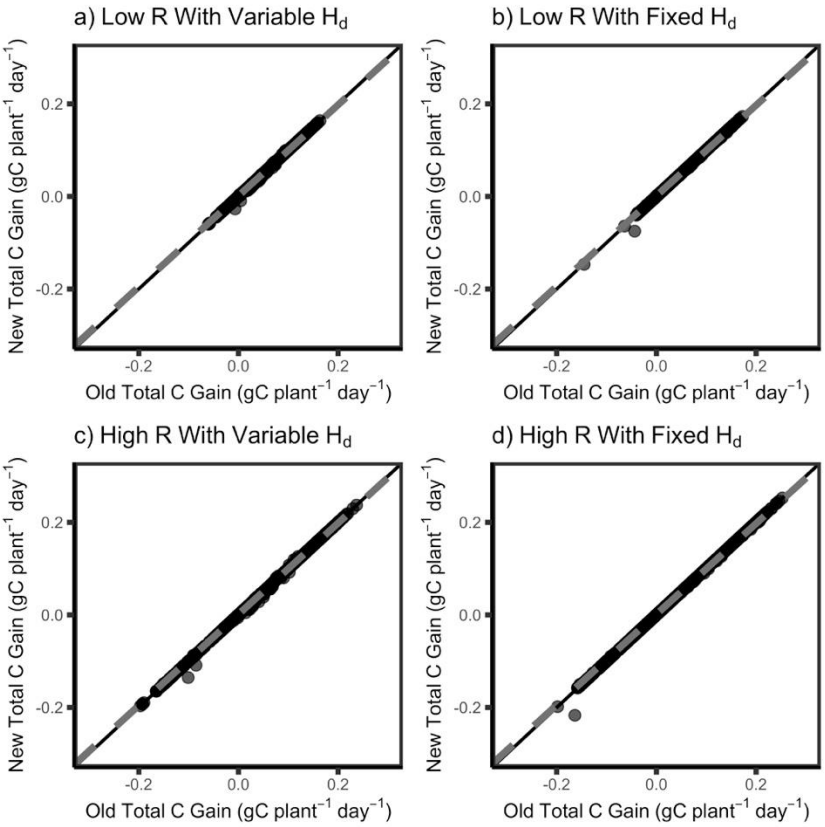


**Figure 6 – The modified Arrhenius equation with the missing term (Equation 10) gives slight differences in modeled total carbon gain compared to Equation 3 for low R (a,b) and high R (c,d) under scenarios where $H_d$ is allowed to vary (a, c) and is fixed to 200 kJ $mol^{-1}$ (b,d). "New" indicates Equation 10, "Old" indicates Equation 3. C: carbon, Low R: low respiration, High R: high respiration. Black line indicates 1:1 line and grey dashed line indicates respective modeled slopes and intercepts.**

## Discussion

We sought to determine whether the missing term in Equation 3 had a meaningful impact on fitted temperature response parameters due to its prevalence in photosynthetic temperature response data and vegetation modeling (Kattge & Knorr, 2007; Duursma & Medlyn, 2012; Rogers et al., 2017; Smith & Dukes, 2017; Stinziano et al., 2018; Stinziano et al., 2019; Kumarathunge et al., 2019). Our present analysis suggests that there is no large impact on the fitted temperature response parameters for $V_{cmax}$ and $J_{max}$, with differences ranging between 0 and 3.8% depending on the parameter. In general, fitting Equation 10 instead of Equation 3 results in slightly reduced values for $E_a$ and $\Delta S$, with essentially no impact for $k_{25}$ and $H_d$ when $H_d$ is fit. When $H_d$ is fixed, there are no meaningful differences in the fits except for $\Delta S$ for $J_{max}$, where Equation 10 values are ~4% lower than Equation 3 values, and intercepts in the $E_a$ regressions of ~-2 kJ $mol^{-1}$, which represents <5% differences between the two equations in most instances. These findings are promising in that one of the parameters to which modelled carbon gain is particularly sensitive, $H_d$ (Stinziano et al., 2018), is minimally affected by the missing term. However, since temperature responses are non-linear, small changes in the shape of an accelerating curve can have a strong impact on the integral of the response (Jensen, 1906). This caused the differences in temperature response parameters to cause ~1.5 – 2.2% difference in daily C balance. The daily C balance was most affected by the missing term in Equation 3 when comparing models where $H_d$ was fixed, leading to a 2.2% change. Overall, comparisons of low-respiration to high-respiration scenarios resulted in similar percent changes in daily C balance; however, the variation was consistently larger under high-respiration across all variables measured. Similar trends were found when comparing differences in daily photosynthesis and A/R.

Based on the above analysis, the impact of the missing term in the modified Arrhenius equation may appear negligible based on the parameter outputs. However given that carbon balance is the time integral of net $CO_2$ assimilation, this may lead to substantial impacts over a long time period. It is thus possible that the apparently small differences we observed could accumulate to relatively large carbon flux errors across large spatial and temporal scales with fluctuating temperatures. A growing body of literature on using Optimality Theory for estimating $V_{cmax25}$ and $J_{max25}$ (Ali et al., 2016; Walker et al., 2017; Smith et al., 2019) still relies on Equation 3 for temperature scaling. Given the impacts we observed, Optimality Theory may be even more successful if the temperature scaling were done

either with Equation 10, or, as we recommend, macromolecular rate theory which is better grounded in thermodynamics (e.g. Hobbs et al., 2013; Liang et al., 2018).

Since Equation 3 is incorrect, there are three arguments to support moving beyond the modified Arrhenius paradigm: 1) there are new approaches to modeling biological temperature responses that are better-grounded in thermodynamics (e.g. Macromolecular Rate Theory; Hobbs et al., 2013; Liang et al., 2018); 2) uncertainties in model outputs may accumulate due to the missing term across large spatial and temporal scales, and 3) the modified Arrhenius model as implemented is categorically incorrect due to a missing term. Therefore, we conclude that future modeling efforts should move beyond this incorrect paradigm.

**Acknowledgments**

We would like to thank Wesley J. Noe at the University of New Mexico for providing climate data. This research was supported by personal funds.

**Additional Information**

A version of this manuscript was posted on bioRxiv (manuscript ID: BIORXIV/2020/921973).

**References**

Ali AA, Xu C, Rogers A, Fisher RA, Wullschleger SD, Massoud EC, Vrugt JA, Muss JD, et al. 2016. A global scale mechanistic model of photosynthetic capacity (LUNA V1.0). Geoscientific Model Development 9:587-606.

Amthor JS. 2000. Direct effect of elevated CO2 on nocturnal in situ leaf respiration in nine temperate deciduous tree species is small. Tree Physiology 20: 139–144.

Arrhenius S. 1915. Quantitative laws in biological chemistry. Bell: London.

Atkin OK, Tjoelker MG. 2003. Thermal acclimation and the dynamic response of plant respiration to temperature. Trends in Plant Science 8:343-351.

Ayub G, Smith RA, Tissue DT, Atkin OK. 2011. Impacts of drought on leaf respiration in darkness and light in *Eucalyptus saligna* exposed to industrial-age atmospheric $CO_2$ and growth temperature. New Phytologist 190: 1003-1018.

356 Bernacchi CJ, Singsaas EL, Pimentel C, Portis Jr AR, Long SP. 2001. Improved temperature response
357 functions for models of rubisco-limited photosynthesis. Plant Cell and Environment 24:253-259.
358 Ciais P, Sabine C, Bala G, Bopp L, Brovkin V, Canadell J, Chhabra A, DeFries R, Galloway J, Heimann M.
359 2013. Carbon and Other Biogeochemical Cycles. In: Heinze C, Tans P, Vesala T, eds. Climate
360 Change 2013: The Physical Science Basis. Cambridge, UK, and New York, NY, USA: Cambridge
361 University Press.
362 Duursma RA, Medlyn BE. 2012. MAESPA: a model to study interaction between water limitation,
363 environmental drivers and vegetation function at tree and stand levels, with an example
364 application to [$CO_2$] x drought interactions. Geoscientific Model Development 5:919-940.
365 Elzhov TV, Mullen KM, Spiess A-N, Bolker B. 2016. minpack.lm: R Interface to the Levenberg-
366 Marquardt nonlinear least-squares algorithm found in MINPACK, plus support for bounds. R
367 package version 1.2-1. https://CRAN.R-project.org/package=minpack.lm
368 Farquhar GD, et al. 1980. A biochemical model of photosynthetic $CO_2$ assimilation in leaves of $C_3$
369 species. Planta 149: 78-90.
370 Harley PC, Sharkey TD. 1991. An improved model of $C_3$ photosynthesis at high CO2: reversed O2
371 sensitivity explained by lack of glycerate re-entry into the chloroplast. Photosynthesis Research
372 27:169-178.
373 Heskel MA, O'Sullivan OS, Reich PB, Tjoelker MG, Weerasinghe LK, Penillard A, Egerton JJG, et al.
374 2016. Convergence in the temperature response of leaf respiration across biomes and plant
375 functional types. Proceedings of the National Academy of Sciences USA 113: 3832-3837.
376 Hobbs JK, Jiao W, Ester AD, Parker EJ, Schipper LA, Arcus VL. 2013. Change in heat capacity for enzyme
377 catalysis determines temperature dependence of enzyme catalyzed rates. ACS Chemical Biology
378 8:2388-2392.
379 Jensen JLWV. 1906. Sur les fonctions convexes et les inégalités entre les valeurs moyennes. Acta
380 Mathematica 30: 175-193.
381 Johnson FH, Eyring H, Williams RW. 1942. The nature of enzyme inhibitions in bacterial luminescence:
382 sulfanilamide, urethane, temperature and pressure. Journal of Cellular and Comparative
383 Physiology 20:247-268.
384 Kattge J, Knorr W. 2007. Temperature acclimation in a biochemical model of photosynthesis: a
385 reanalysis of data from 36 species. Plant, Cell & Environment 30:1176-1190.

Kruse J, Hopmans P, Adams MA. 2008. Temperature responses are a window to the physiology of dark respiration: differences between $CO_2$ release and $O_2$ reduction shed light on energy conservation. Plant, Cell Environment 31: 901-914.

Kumarathunge DP, Medlyn BE, Drake JE, Tjoelker MG, Aspinwall MJ, Battaglia M, Cano FJ, Carter KR, Molly AC, Lucas AC, et al. 2019. Acclimation and adaptation components of the temperature dependence of plant photosynthesis at the global scale. New Phytologist 222:768-784.

Kumarathunge DP, Medlyn BE, Drake JE, Tjoelker MG, Aspinwall MJ, Battaglia M, Cano FJ, Carter KR, Molly AC, Lucas AC, et al. 2018. ACi-TGlob_V1.0: a global dataset of photosynthetic $CO_2$ response curves of terrestrial plants. doi: 10.6084/m9.figshare.7283567.v1.

Liang LL, Arcus VL, Heskel MA, O'Sullivan OS, Weerasinghe LK, Creek D, Egerton JJG, et al. 2018. Macromolecular rate theory (MMRT) provides a thermodynamics rationale to underpin the convergent temperature response in plant leaf respiration. Global Change Biology 24:1538-1547.

Medlyn BE, Duursma RA, Eamus D, Ellsworth DS, Prentice IC, Barton CVM, Crous KY, et al. 2011. Reconciling the optimal and empirical approaches to modelling stomatal conductance. Global Change Biology 17:2134-2144.

Medlyn BE, Dreyer E, Ellsworth D, Forstreuter M, Harley PC, Kirschbaum MUF, Le Roux X, et al. 2002. Temperature responses of parameters of a biochemically based model of photosynthesis. II. A review of experimental data. Plant, Cell & Environment 25:1167-1179.

Norman JM, Campbell GS. 1998. An introduction to environmental biophysics. New York NY: Springer.

R Core Team. 2019. R: A language and environment for statistical computing. R Foundation for Statistical Computing, Vienna, Austria. URL https://www.R-project.org/.

Rogers A, Medlyn BE, Dukes JS, Bonan G, von Caemmerer S, Dietze MC, Kattge J, et al. 2017. A roadmap for improving the representation of photosynthesis in Earth system models. New Phytologist 213:22-42.

Sharkey TD. 1985. Photosynthesis in intact leaves of $C_3$ plants – physics, physiology and rate limitations. Botanical Review 51:53-105.

Smith NG, Dukes JS. 2017. Short-term acclimation to warmer temperatures accelerates leaf carbon exchange processes across plant types. Global Change Biology 23:4840-4853.

Smith NG, Keenan TF, Prentice IC, Wang H, Wright IJ, Niinemets Ü, Crous KY, Domingues TF, et al. 2019. Global photosynthetic capacity is optimized to the environment. Ecology Letters 22:506-517.

Stinziano JR, Murphy BK. 2020. arrhenius.comparison: comparing versions of the modified Arrhenius equation. R package version 1.0.0.

Stinziano JR, Way DA. 2017. Autumn photosynthetic decline and growth cessation in seedlings of white spruce are decoupled under warming and photoperiod manipulations. Plant, Cell and Environment 40:1296-1316.

Stinziano JR, Way DA, Bauerle WL. 2018. Improving models of photosynthetic thermal acclimation: which parameters are most important and how many should be modified? Global Change Biology 24:1580-1598.

Stinziano JR, Bauerle WL, Way DA. 2019. Modelled net carbon gain responses to climate change in boreal trees: impacts of photosynthetic parameter selection and acclimation. Global Change Biology 25:1445-1465.

Walker AP, Quaife T, van Bodegom PM, De Kauwe MG, Keenan TF, Joiner J, Lomas MR, MacBean, et al. 2017. The impact of alternative trait-scaling hypotheses for the maximum photosynthetic carboxylation rate ($V_{cmax}$) on global gross primary production. New Phytologist 215:1370-1386.

Way DA, Yamori W. 2014. Thermal acclimation of photosynthesis: on the importance of adjusting our definitions and accounting for thermal acclimation of respiration. Photosynthesis Research 119:89-100.

Weger HG, Guy RD. 1991. Cytochrome and alternative pathway respiration in white spruce (*Picea glauca*) roots. Effects of growth and measurement temperature. Physiologia Plantarum 83:675-681.

**Supplementary Information**

*Instructions for installing {arrhenius.comparison} in R for review purposes*

1. Download the arrhenius.comparison.tar.gz file
2. Set working directory in R to the directory that holds the arrhenius.comparison.tar.gz file using setwd()
3. Run:

   install.packages("arrhenius.comparison_1.0.0.tar.gz", repos = NULL, type = "source")

   library(arrhenius.comparison)